



The heparin-binding hemagglutinin protein of *Mycobacterium tuberculosis* is a nucleoid-associated protein

Received for publication, August 8, 2023, and in revised form, October 5, 2023. Published, Papers in Press, October 19, 2023.
<https://doi.org/10.1016/j.jbc.2023.105364>

Chetkar Chandra Keshavam¹, Saba Naz^{1,2}, Aanchal Gupta³, Priyadarshini Sanyal^{2,4}, Manisha Kochar^{1,3} , Aakriti Gangwal¹, Nitika Sangwan¹, Nishant Kumar¹, Ekta Tyagi¹, Simran Goel¹, Nitesh Kumar Singh² , Divya Tej Sowpati², Garima Khare⁵, Munia Ganguli³, Dominique Raze⁶, Camille Locht⁶, Sharmila Basu-Modak¹, Meetu Gupta^{3,*}, Vinay Kumar Nandicoori^{2,4,7,*}, and Yogendra Singh^{1,8,*}

From the ¹Department of Zoology, University of Delhi, Delhi, India; ²CSIR-Centre for Cellular and Molecular Biology, Hyderabad, India; ³CSIR-Institute of Genomics and Integrative Biology, New Delhi, India; ⁴Academy of Scientific and Innovative Research (AcSIR), CSIR- Centre for Cellular and Molecular Biology (CSIR-CCMB) Campus, Hyderabad, India; ⁵Department of Biochemistry, University of Delhi South Campus, New Delhi, India; ⁶Univ. Lille, CNRS, Inserm, CHU Lille, Institut Pasteur de Lille, U1019 - UMR9017 - CIL - Centre for Infection and Immunity of Lille, Lille, France; ⁷National Institute of Immunology, Aruna Asaf Ali Marg, New Delhi, India; ⁸Delhi School of Public Health, Institution of Eminence, University of Delhi, Delhi, India

Reviewed by members of the JBC Editorial Board. Edited by Chris Whitfield

Nucleoid-associated proteins (NAPs) regulate multiple cellular processes such as gene expression, virulence, and dormancy throughout bacterial species. NAPs help in the survival and adaptation of *Mycobacterium tuberculosis* (*Mtb*) within the host. Fourteen NAPs have been identified in *Escherichia coli*; however, only seven NAPs are documented in *Mtb*. Given its complex lifestyle, it is reasonable to assume that *Mtb* would encode for more NAPs. Using bioinformatics tools and biochemical experiments, we have identified the heparin-binding hemagglutinin (HbhA) protein of *Mtb* as a novel sequence-independent DNA-binding protein which has previously been characterized as an adhesion molecule required for extrapulmonary dissemination. Deleting the carboxy-terminal domain of HbhA resulted in a complete loss of its DNA-binding activity. Atomic force microscopy showed HbhA-mediated architectural modulations in the DNA, which may play a regulatory role in transcription and genome organization. Our results showed that HbhA colocalizes with the nucleoid region of *Mtb*. Transcriptomics analyses of a *hbhA* KO strain revealed that it regulates the expression of ~36% of total and ~29% of essential genes. Deletion of *hbhA* resulted in the upregulation of ~73% of all differentially expressed genes, belonging to multiple pathways suggesting it to be a global repressor. The results show that HbhA is a nonessential NAP regulating gene expression globally and acting as a plausible transcriptional repressor.

The linear size of bacterial genomic DNA is much larger than the bacterial cell itself. Hence, fitting the genome within a cell is a challenging task. Genetic material needs to be

compacted efficiently (1000 times) (1) along with maintaining its availability to the protein machinery, regulating various cellular processes such as DNA replication, transcription, and repair. Unlike eukaryotes, these processes occur simultaneously in prokaryotes. Thus, the confined bacterial genome, known as a nucleoid, remains constantly in a dynamic state during the cell cycle (2–4). The dynamicity of the bacterial genome is maintained by histone-like proteins known as nucleoid-associated proteins (NAPs) (5–8). NAPs are small, basic proteins associated with the bacterial chromosome, and their expression varies during different stages of growth (9). NAPs compact genomic DNA into microdomains as independent topological domains of ~10 kb (10). Compaction of genomic DNA is facilitated by either bending or wrapping of DNA (HU, IHF, Fis, and Dps) or by bridging of DNA (H-NS) (5, 11). NAPs regulate multiple key cellular processes, such as transcription of genes involved in virulence and general physiology (H-NS, IHF, HU, and EspR) (6, 12–14), DNA replication (HU, IHF, and Fis) (15, 16), recombination and DNA repair (HU) (17). The number of NAPs varies among bacterial species. For example, *Escherichia coli* has at least 14 NAPs (18–20), whereas *Mtb* has only seven identified NAPs (21, 22). Considering the complex lifestyle of this pathogen, the number of identified NAPs and their described roles appear far less.

The physiological significance of NAPs in *Mtb* survival and virulence has been reported in several studies. For example, HupB is essential for the survival of *Mtb* within macrophages (23), protection of DNA from damaging agents (24), DNA repair (25), and antibiotic tolerance (26). Lsr2 is essential for survival, required for the growth of *Mtb* under normoxic, hyperoxic, and anaerobic conditions (27), protection against oxidative stress (28), isoniazid and ethambutol tolerance (29), and biofilm formation (30). EspR regulates the expression of genes involved in the typeVII secretion system that controls the secretion of many important virulence determinants of this pathogen (31), and other genes involved in survival and

Present Address for Simran Goel: Department of Molecular Cell Biology, Institute of Biochemistry and Pathobiochemistry, Ruhr University Bochum, Germany.

* For correspondence: Yogendra Singh, ysinghdu@gmail.com; Vinay Kumar Nandicoori, vinaykn@ccmb.res.in; Meetu Gupta, meetug80@gmail.com.

HbhA is a DNA-binding protein of *M. tuberculosis*

virulence, including genes involved in phthiocerol dimycoserolate biosynthesis (14). Another NAP, mycobacterial integration host factor (mIHF), the third most abundant protein in *Mtb*, is critical for *in vitro* growth (32–34), regulates DNA and protein synthesis, including expression of housekeeping and virulence genes (33). NapM contributes to the pathogen's survival inside macrophages during infection and in various stress conditions (35) and is involved in antibiotic tolerance (36). NapA, a recently characterized NAP from *Mtb* has been shown to regulate the expression of an operon containing genes involved in virulence (21). Based on the underrepresentation of identified NAPs and the presence of many uncharacterized genes in *Mtb*, we searched for the unidentified NAPs in *Mtb* proteome. We have identified heparin-binding hemagglutinin (HbhA) as a sequence-independent DNA-binding protein and have studied its potential role in chromatin condensation and regulation of gene expression.

Results

HbhA from *Mtb* is a small, basic histone-like protein

Earlier studies have shown that lysine-rich repeats (Fig. 1A) in histone H1 isoforms are associated with their DNA-binding activity (37, 38). Therefore, to identify *Mtb* NAPs, we searched for these repeats in the *Mtb* proteome. BLAST analysis of *Mtb* proteome predicted the presence of two motifs (AAKK and AKKA) in various mycobacterial proteins. Two AAKK repeats are present in HupB and HbhA, and seven AKKA repeats are present in HupB and five in HbhA (Fig. 1B). The AKKA repeat motifs are also present in RplV (4 repeats), and Rv3852 (3 repeats) (Fig. 1B). HupB and Rv3852 have been already established as NAPs (39, 40), while the RplV protein binds specifically to 23S rRNA (<https://mycobrowser.epfl.ch/genes/Rv0706>). The presence of the AKKA motifs in the amino acid sequences of HbhA (Fig. 1C) and RplV (Fig. 1D) suggests that these proteins could act as NAPs. Further, the basic isoelectric point (pI-9.8 and 12.3) and small size (21.5 kDa and 20.4 kDa) of HbhA (<https://mycobrowser.epfl.ch/genes/Rv0475>) and RplV (<https://mycobrowser.epfl.ch/genes/Rv0706>) are consistent with their putative role as NAPs. We first examined the sequence-independent DNA-binding activity of RplV with supercoiled and linear forms of pUC19 DNA in an agarose gel-based mobility shift assay. The absence of a shift in the mobility pattern of pUC19 DNA in the presence of RplV (Fig. 1E left panel) indicated that RplV does not possess sequence-independent DNA-binding property, a hallmark feature of NAPs (6). In contrast, Lsr2, a well-characterized *Mtb* NAP (41), showed efficient binding with pUC19 DNA (Fig. 1E right panel). Glutathione S-transferase (GST) and Lsr2 were used as negative and positive controls, respectively. This shows that RplV does not belong to the NAPs family. Multiple sequence alignments of HbhA from various mycobacterial species and actinomycetes using CLUSTAL Omega (<https://www.ebi.ac.uk/Tools/msa/clustalo/>) showed that HbhA is highly conserved in actinomycetes (Fig. S1, A and B). HbhA from pathogenic mycobacterial species has been

shown to act as an adhesin and is responsible for extrapulmonary dissemination of *Mtb* (42, 43).

HbhA binds to DNA in a sequence-independent manner

To evaluate the nonspecific DNA binding ability of HbhA, we performed EMSAs using pUC19 DNA as a nonspecific DNA probe. pUC19 DNA was selected due to its high AT content since NAPs bind preferentially to AT-rich DNA (6). It has been previously reported that histone-like proteins show a higher preference for binding with supercoiled DNA than to linear DNA (44, 45). Therefore, we performed EMSAs using supercoiled and linear forms of pUC19 plasmid DNA. EMSAs were performed by incubating a constant amount of DNA with varying amounts of HbhA. We observed comparable mobility shifts with supercoiled and linear pUC19 DNA with increasing amounts of HbhA (Fig. 2, A and B). We also observed that HbhA forms multiple DNA-protein complexes in a concentration-dependent manner (Fig. 2, A and B). These observations indicate a complex much larger than expected by the association of a single molecule of HbhA with plasmid DNA, suggesting the binding of multiple HbhA molecules with a single DNA molecule in a sequence-independent fashion (Fig. 2, A and B). GST and Lsr2 were used as the negative and positive controls, respectively.

The C-terminal domain of HbhA is required for DNA binding

Earlier studies have revealed the presence of three functional domains in HbhA: a hydrophobic domain of 18 amino acid residues in the N-proximal region of the protein, an α -helical coiled-coil domain of 81 amino acid residues and a C-terminal domain (161–199 amino acid residues) which is rich in Lys-Pro-Ala residues (42, 46–48). We observed the presence of five repeats of the AKKA motif in the C-terminal domain of HbhA (Fig. 1C). As the presence of AKKA and several similar motifs in histones and NAPs has been linked to their DNA-binding abilities (24, 37, 38, 40, 49–52), we investigated the role of AKKA motifs in the DNA-binding activity of HbhA. We, therefore, constructed a mutant with a C-terminal deletion (HbhA Δ C) and two mutants with N-terminal deletions (HbhA₁₅₁₋₁₉₉ and HbhA₁₆₁₋₁₉₉) (Fig. 2C). We observed a complete loss in the mobility shifts of pUC19 DNA in the presence of HbhA Δ C (Fig. 2D). In contrast, mobility shifts of pUC19 DNA were observed in the presence of HbhA₁₅₁₋₁₉₉ and HbhA₁₆₁₋₁₉₉ and were comparable to that of HbhA (Fig. 2D). To rule out the possibility of mutation-induced structural alterations in HbhA Δ C, circular dichroism spectra were determined to examine the secondary structures of HbhA and HbhA Δ C. Superimposed spectra of HbhA and HbhA Δ C showed similar patterns (Fig. 2E). These results indicate that the C-terminal domain of HbhA containing AKKA repeat motifs is responsible for its DNA-binding activity.

HbhA binding to DNA leads to DNA looping and bending

Histones and histone-like proteins protect DNA from degradation by DNA-damaging agents such as DNaseI (24, 29, 53–55). To test whether HbhA binding to DNA results in

A

| DNA-binding Motifs | Number of Repeats | Histone H1 isoforms |
|--------------------|-------------------|---------------------|
| S/TPKK | 3 | H1d |
| AAKK/AKKA | 5 | H1d |
| PKAAKP | 2 | H1d |
| K/RPK/R | 6, 2 | H1d, H1t |

(Adapted from Khadake JR *et al.*, 1995)

B

| DNA-binding Motifs | Proteins having specific DNA-binding motifs | Number of Repeats |
|--------------------|---|-------------------|
| S/TPKK | - | - |
| AAKK/AKKA | HupB, HbhA/ HupB, HbhA, RplV, Rv3852 | 2, 2/ 7, 5, 4, 3 |
| PKAAKP | - | - |
| K/RPK/R | - | - |

C

***Mycobacterium tuberculosis* H37Rv|Rv0475|HbhA**

MAENSNIDDIKAPLLAALGAADLALATVNELITNLRERAETRTDTRSRVEESRARLTKLQEDLPEQL
 TELREKFTAEEELRKAAGYLEAATSRYNELVERGEAALERLRSQQSFEEVSARAEGYVDQAVELTQ
 EALGTVASQTRAVGERAAKLVGIELPKKAAPAKKAAPAKKAAPAKKAAAKKAPAKKAAAKKVTQK

166 169 172 175 178 181 183 186 188 191

D

***Mycobacterium tuberculosis* H37Rv|Rv0706|RplV**

MTAATKATEYPSAVAKARFVRVSPRKARRVIDLVRGRSVSDALDILRWAPQAASGPVAKVIASAAAN
 AQNNGGLDPATLVATVYADQGPTAKRIRPRAQQGRAFRIRRRTSHITVVVESRPAKDQRSACKSSRA
 RRTEASKAASKVGATAPAKKAAAKAPAKKAPASSGVKKTPAKKAAPAKKAPAKASETSAAKGGSD

151 154 160 163 174 177 179 182

E

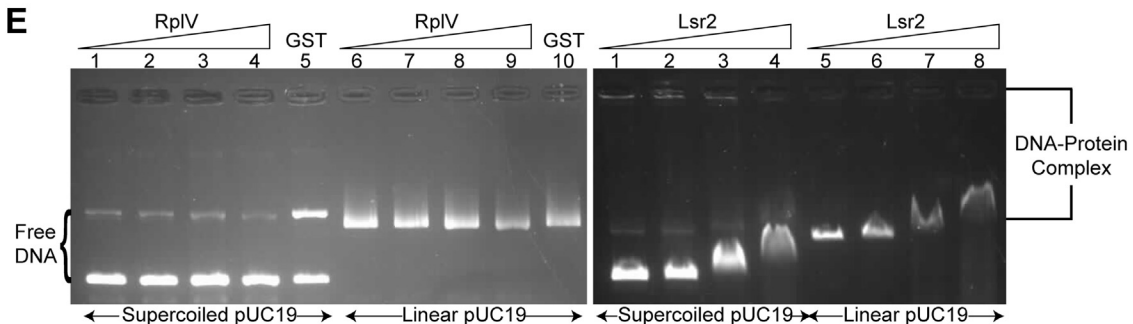


Figure 1. *In-silico* identification of HbhA from *Mtb* as a putative NAP. A, list of motifs that govern the DNA-binding ability of Histone H1 isoforms. B, presence of specific DNA-binding motifs in the amino acid sequence of different proteins encoded in the genome of *Mtb* and the number of repeats of DNA-binding motifs. C and D, the amino acid sequence of HbhA (C) and RplV (D) from *Mtb* shows the position of AKKA motifs. AKKA motifs are highlighted in red, and their positions are written in plum. Green highlighted portion of the amino acid sequence in (C) represents the C-terminal domain of HbhA. E, sequence- and structure-independent DNA-binding activity of RplV. A constant amount of supercoiled and linear forms of pUC19 DNA were incubated with

HbhA is a DNA-binding protein of *M. tuberculosis*

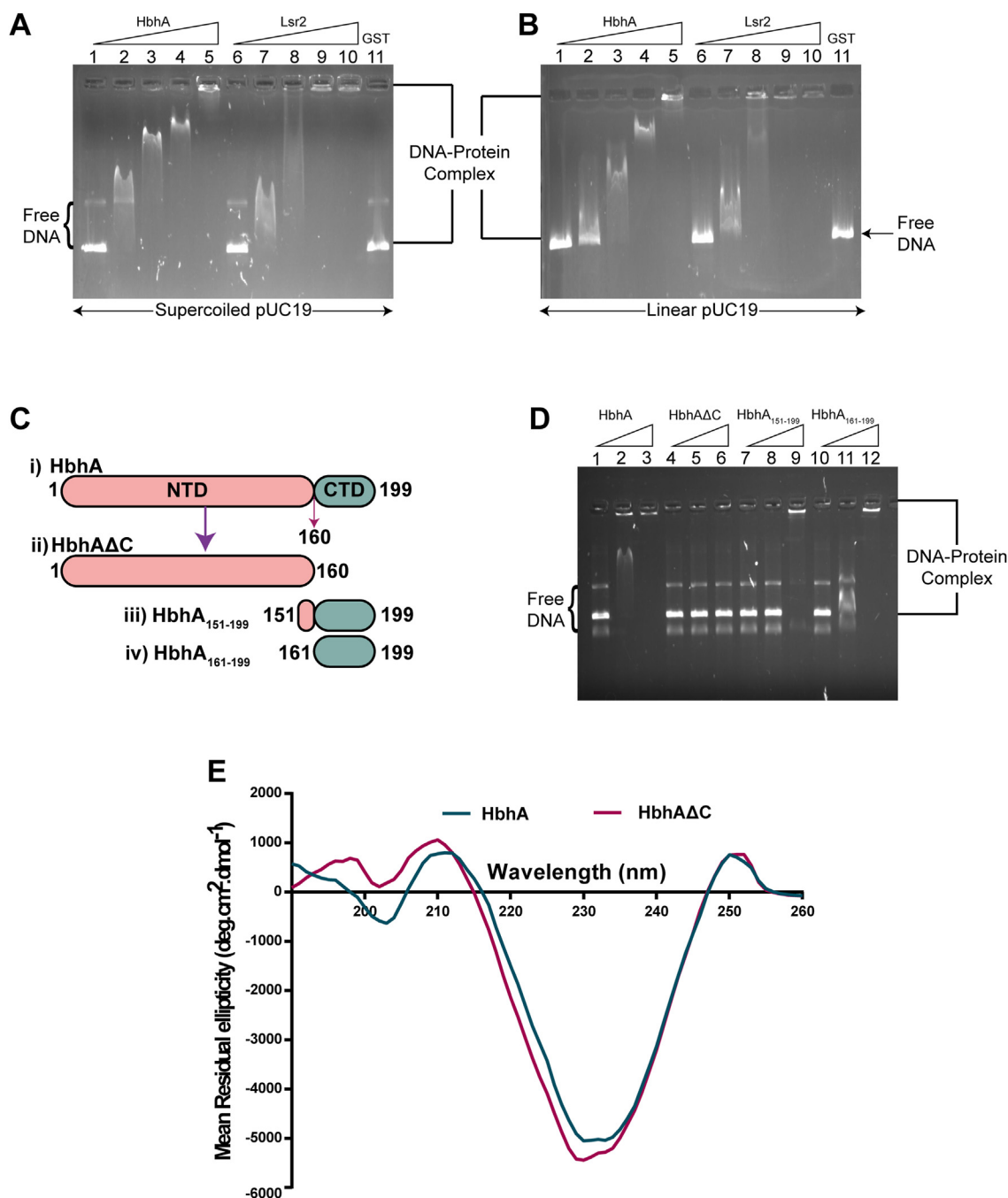


Figure 2. HbhA from *Mtb* binds to DNA in a sequence- and structure-independent manner, and its C-terminal domain is DNA-binding domain. *A* and *B*, binding of HbhA with supercoiled and linear forms of pUC19 DNA, respectively. Constant amount of supercoiled and linear forms of pUC19 DNA were incubated with increasing molar ratios (1:0, 1:100, 1:250, 1:500, and 1:1000) of HbhA (lanes 1–5) and Lsr2 (lanes 6–10) with respect to pUC19. Lsr2 was used as a positive control and GST (lane 11) at a DNA:protein molar ratio of 1:1000 was used as a negative control. *C*, an illustration representing the generation of a C-terminal deleted mutant (HbhA Δ C) and two N-terminal domain deleted mutants (HbhA₁₅₁₋₁₉₉ and HbhA₁₆₁₋₁₉₉) of HbhA. NTD and CTD represents N-terminal and C-terminal domains, respectively. *D*, constant amount of supercoiled pUC19 DNA were incubated with increasing DNA:protein molar ratios (1:0, 1:100, and 1:1000) of HbhA (lanes 1–3), HbhA Δ C (lanes 4–6), HbhA₁₅₁₋₁₉₉ (lanes 7–9), and HbhA₁₆₁₋₁₉₉ (lanes 10–12) with respect to pUC19. Native DNA and DNA-protein complexes were resolved on 0.5% agarose gel and visualized using EtBr staining. *E*, CD spectra of HbhA and HbhA Δ C. CTD, C-terminal domain; EtBr, ethidium bromide; GST, glutathione S-transferase; HbhA, heparin-binding hemagglutinin; NTD, N-terminal domain.

protection from DNaseI, we incubated HbhA with 500 ng of supercoiled pUC19 DNA in an increasing DNA:protein molar ratio, followed by treatment with 1 U of DNaseI. In the

absence of HbhA, treatment of pUC19 DNA with DNaseI resulted in degradation of DNA, while in its presence, increased protection was observed with increasing

increasing molar ratios (1:0, 1:50, 1:250, and 1:500) of RplV and Lsr2. Lsr2 was used as a positive control. GST at a DNA:protein molecular ratio of 1:500 was used as a negative control. GST, glutathione S-transferase; HbhA, heparin-binding hemagglutinin; *Mtb*, *Mycobacterium tuberculosis*.

DNA:protein molar ratios with almost complete protection at the 1:1000 molar ratio (Fig. 3A). These results indicate that HbhA protects DNA from DNaseI degradation.

Histone and other NAPs are involved in the *in-vitro* transcription regulation (56, 57). Lsr2, a known nucleoid-associated protein from *Mtb*, has also been shown to inhibit *in-vitro* transcription using T7 promoter system (29). To check whether HbhA could be a transcriptional regulator, we measured the *in-vitro* transcription regulatory activities of HbhA and observed that HbhA inhibits transcription, while HbhAΔC failed to inhibit transcription (Fig. 3B). Histone-like proteins are known to modulate the topological features of DNA in the presence of topoisomerase (21, 29, 44, 58, 59). To determine whether HbhA can also perform such a function, we incubated pUC19 DNA with topoisomerase I to relax the supercoiled DNA and added HbhA. We observed that HbhA enhanced the relaxation activity of topoisomerase I (Fig. 3C).

To gain further insight into any possible conformational changes in the DNA induced by the binding of HbhA, we used atomic force microscopy. We observed HbhA-induced changes in linear and supercoiled plasmid DNA morphology. At various regions, it is observed that the DNA bound to HbhA proteins appeared as beads on string structure (bright areas indicated by blue arrows in Fig. 3, D and E). In some regions, there was looping (cyan arrow) and bending (lavender arrow) of the DNA as well (Fig. 3, D and E). This is likely induced by the nonspecific binding of HbhA, since it appears to be randomly bound on the DNA filaments. Without HbhA, the DNA appears as filaments with uniform height (Fig. 3, D and E, upper panels). No conformational changes in the DNA occurred in the presence of HbhAΔC (Fig. S2A). Lsr2 was used as a positive control for these experiments, showing that Lsr2 causes bridging of the linear DNA strands (Fig. S2B), as reported previously (60).

HbhA deletion has no impact on *in vitro* growth of *Mtb*

Next, we determined whether HbhA colocalizes with the nucleoid. *Mtb* nucleoids were isolated using sucrose density gradient centrifugation, and the concentration of DNA was measured in the various fractions (Fig. 4A). Fractions containing the highest amounts of DNA (Fractions 16 and 17) were considered nucleoid fractions (Fig. 4A) (54). Colocalization of HbhA with nucleoids was examined by immunoblot analyses, and the fractions with the highest amount of DNA were probed with anti-HbhA antibodies for the presence of HbhA. The presence of HbhA in fractions 16 and 17 indicates the colocalization of HbhA with nucleoids (Fig. 4B). To determine the specificity of HbhA-nucleoid colocalization, the presence of a cytosolic protein GroEL2 was also examined and was found absent in the nucleoid fractions (Fig. S3).

To examine the role of HbhA on the growth of *Mtb*, we compared the growth kinetics of WT *Mtb*103 (*MT103*) with those of the *hbhA* deleted strain *MT103ΔhbhA* and the complemented strain *MT103ΔhbhA::hbhA* (Fig. 4C) (43) in nutrient-rich 7H9 medium and nutrient-limiting Sauton's medium. There were no significant differences in the growth

patterns of all three strains (Fig. 4, D and E), indicating that HbhA has no impact on the *in vitro* survival of *Mtb*.

HbhA acts as a global transcriptional regulator

Since NAPs also act as global transcriptional regulators (6), we investigated the possibility of HbhA being a transcriptional regulator. To define the HbhA regulon, the transcriptomes of *MT103* and *MT103ΔhbhA* strains were compared by RNA-sequence analyses of four independent biological replicates (Fig. 5A). Differentially expressed genes (DEGs) were identified using DESeq2 analysis and represented as the volcano plot, where blue and red dots indicate significantly upregulated and downregulated genes, respectively [\log_2 fold change (\log_2fc) >1.0 and adjusted *p*-value (*padj*) < 0.05] (Fig. 5B and Table S1, A and B). A complete set of significantly upregulated and downregulated genes for all four biological replicates of *MT103* and *MT103ΔhbhA* are shown in the heatmap (Fig. 5C). Pathway analysis suggests that DEGs belong to multiple pathways such as virulence, detoxification, adaptation, cell wall synthesis and cell processes, lipid metabolism, and intermediary metabolism and respiration (Fig. 5D). Operonic arrangement analysis of DEGs showed that 38.80% of total DEGs are non-operonic, and 61.20% are operonic genes (Fig. 5E). HbhA deletion resulted in differential expression of a total of 570 genes (\log_2fc > 1.0 and *padj* < 0.05), of which 416 genes (72.98% of total DEGs) were upregulated, and 154 genes (27.02% of total DEGs) were downregulated (Fig. 5F). These results indicate that HbhA is a plausible transcriptional repressor. Of the 570 DEGs, 29 genes (22 operonic and seven non-operonic) were annotated as essential (Fig. 5G). Gene enrichment analysis showed that critical virulence and metabolic pathways such as response to hypoxia, response to copper ion, and cholesterol catabolic processes are significantly enriched in upregulated genes upon deletion of HbhA (Fig. 5H and Table S2, A and B). Biotype analysis showed that ~98% of all DEGs are protein-coding genes (Fig. 5I). By applying a cutoff of $\log_2fc > 0.5$ and *padj* < 0.05, we found that expression of ~36% of the total *Mtb* genes (1444 genes) and ~29% of all essential genes are regulated by HbhA (Table S3, A and B). These results show that HbhA is a novel NAP, although deletion has no impact on *in-vitro* survival.

Discussion

Bacteria can survive through various stress conditions. To cope with the stress, they have acquired numerous group- or species-specific and universal adaptive mechanisms (61–63). Among these mechanisms, modulation in the topology of the entire chromosome or within the specific regions of the chromosome is a ubiquitous, efficient, and effective strategy for adaptation (64–66). Chromosomal topology within bacterial cells is maintained by several factors, including macromolecular crowding, depletion forces, DNA supercoiling, and NAPs (5, 6, 67–70). Using conserved motifs (Fig. 1A) present in histone proteins, we searched for the presence of those motifs in the proteome of *Mtb* and found four proteins (HupB, HbhA, RplV, and Rv3852) (Fig. 1B) out of which two (HupB

HbhA is a DNA-binding protein of *M. tuberculosis*

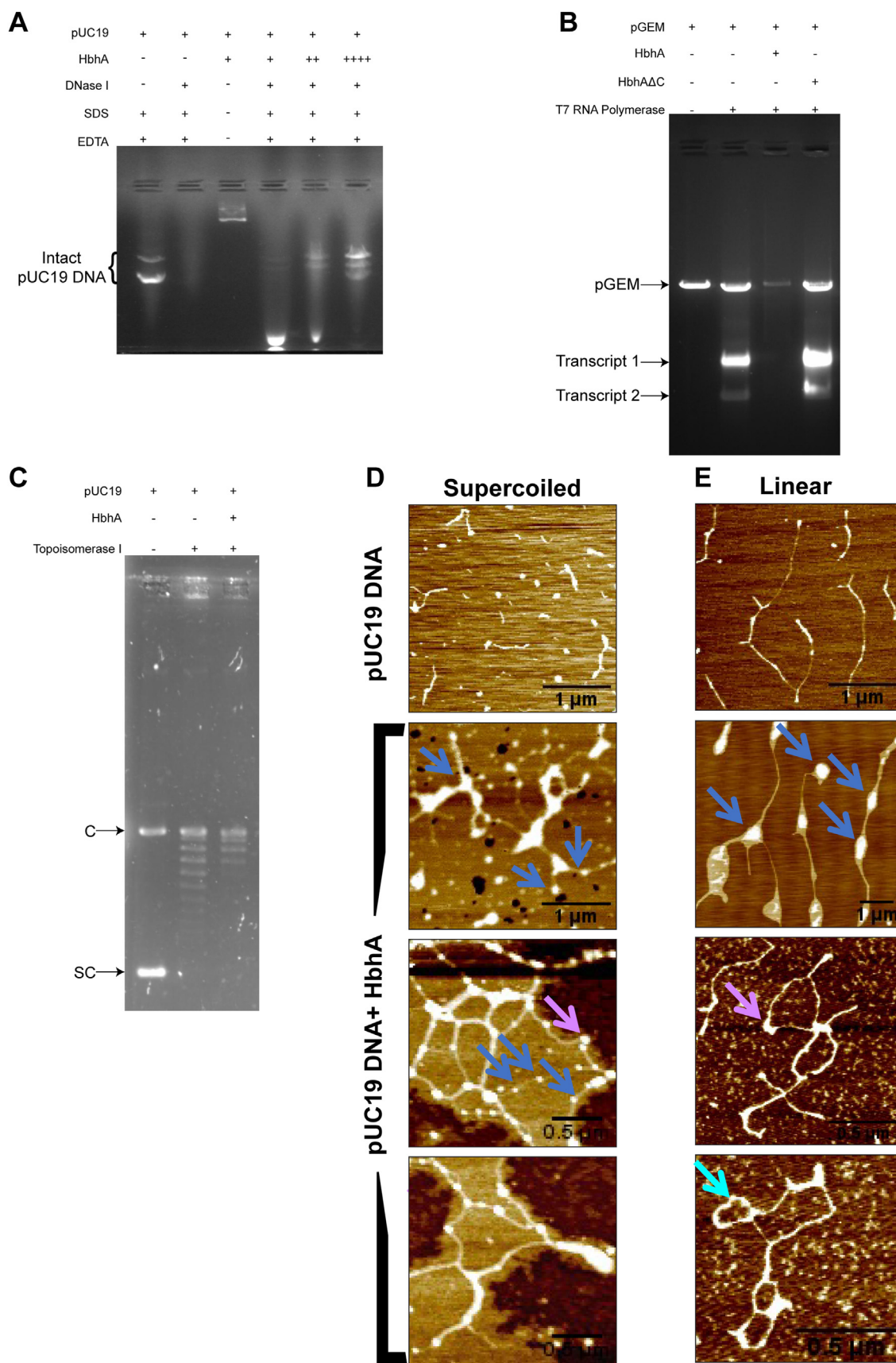


Figure 3. HbhA possesses characteristic features of a NAP. *A*, agarose gel image showing HbhA mediated protection of DNA from DNaseI enzymatic activity. Increasing DNA:HbhA molecular ratios enhanced DNA protection from DNaseI activity. +, ++, and +++ denotes 1:250, 1:500, and 1:1000 DNA:HbhA molar ratios, respectively. *B*, agarose gel image showing inhibitory effect of HbhA on *in vitro* transcription reaction mediated by T7 RNA

HbhA is a DNA-binding protein of *M. tuberculosis*

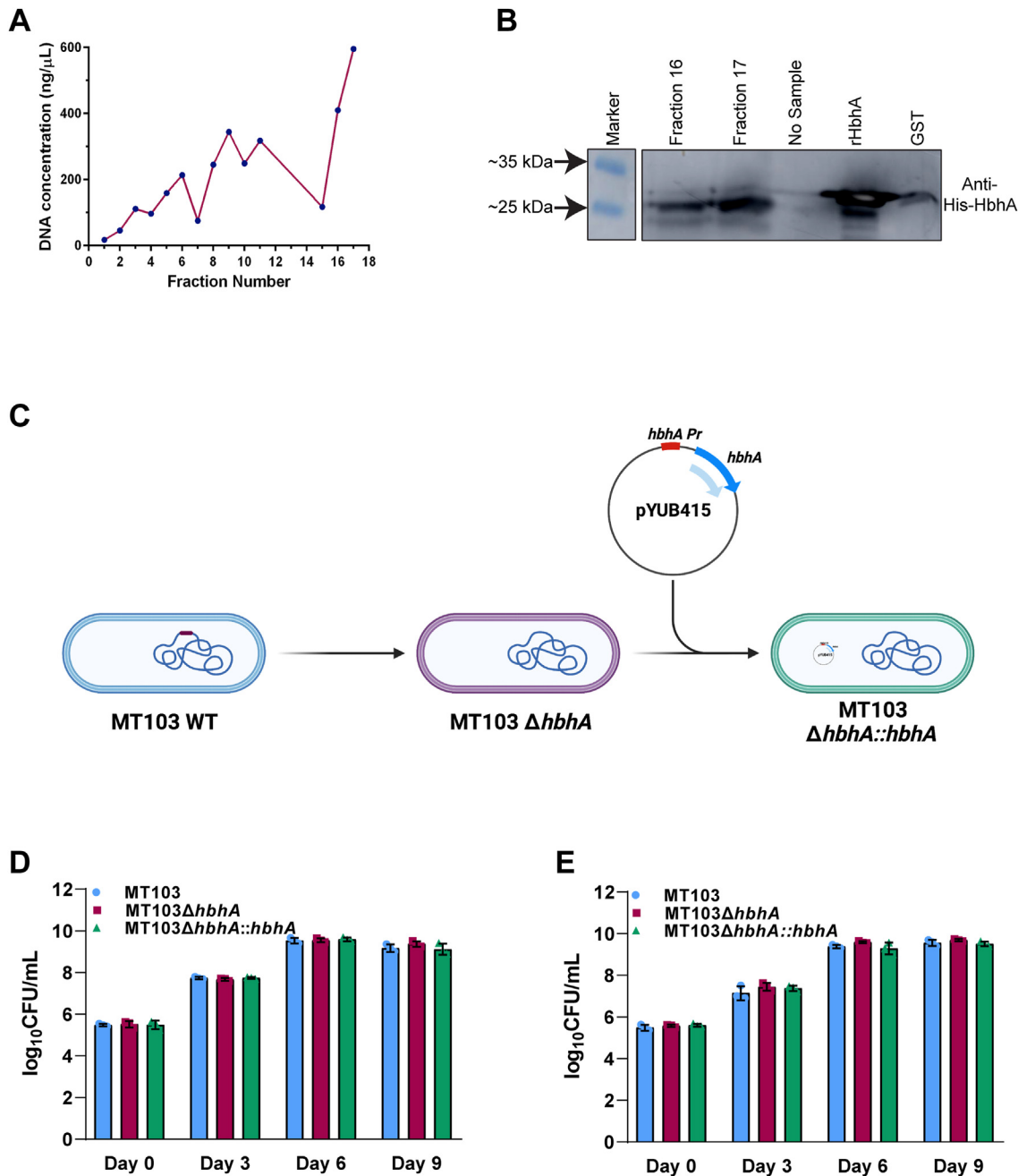


Figure 4. HbhA colocalizes with nucleoid of *Mtb* and is nonessential for *in vitro* growth of *Mtb*. *A*, nucleoids were isolated using 12 to 60% sucrose density gradient centrifugation. DNA concentration (ng/μl) in each fractions of 500 μl were plotted against fraction number in a XY-graph. Fractions with highest DNA content represent the nucleoid fractions. *B*, representative immunoblot of three independent experiments showing the presence of HbhA protein in nucleoid fractions. rHbhA represents His-HbhA recombinant purified protein. The presence of HbhA was detected using antibodies generated in mice against His-HbhA at 1:5000. *C*, a schematic representation of MT103, MT103 $\Delta hbhA$, and MT103 $\Delta hbhA::hbhA$ strains. *D* and *E*, stationary phase cultures of MT103, MT103 $\Delta hbhA$, and MT103 $\Delta hbhA::hbhA$ strains were inoculated at an initial A_{600} of 0.05 in 7H9 (*D*) and Sauton's (*E*) medium. Growth kinetics were measured by enumerating CFUs at indicated time points. Data represented shows mean log₁₀ CFU/ml \pm SD of independent biological triplicates. CFU, colony-forming units; HbhA, heparin-binding hemagglutinin; *Mtb*, *Mycobacterium tuberculosis*.

polymerase. Expected sizes of transcripts 1 and 2 are ~2368 nucleotides and ~1042 nucleotides, respectively. + and - denotes the presence and absence of specific components in the reaction mixture. C, agarose gel image showing the effect of HbhA on topoisomerase I-mediated relaxation of pUC19 DNA. + and - denotes the presence and absence of specific components in the reaction mixture. C and SC denote the covalently closed circular and supercoiled forms of pUC19 DNA, respectively. *D* and *E*, AFM images showing HbhA-mediated architectural modulations in supercoiled and linear forms of pUC19 DNA, respectively. 1:250 DNA::HbhA molar ratio was used to visualize the architectural effect of HbhA on pUC19 DNA. *Upper panel* in (*D* and *E*) denotes supercoiled and linear forms of pUC19 DNA alone, respectively, in 1 \times EMSA buffer. *Blue arrows* denote beads on a string like structure, *lavender arrows* denote bending of DNA molecule, *cyan arrow* denotes looping of DNA molecules. Scale bars are denoted in respective panels. AFM, atomic force microscopy; HbhA, heparin-binding hemagglutinin; NAP, nucleoid-associated proteins.

HbhA is a DNA-binding protein of *M. tuberculosis*

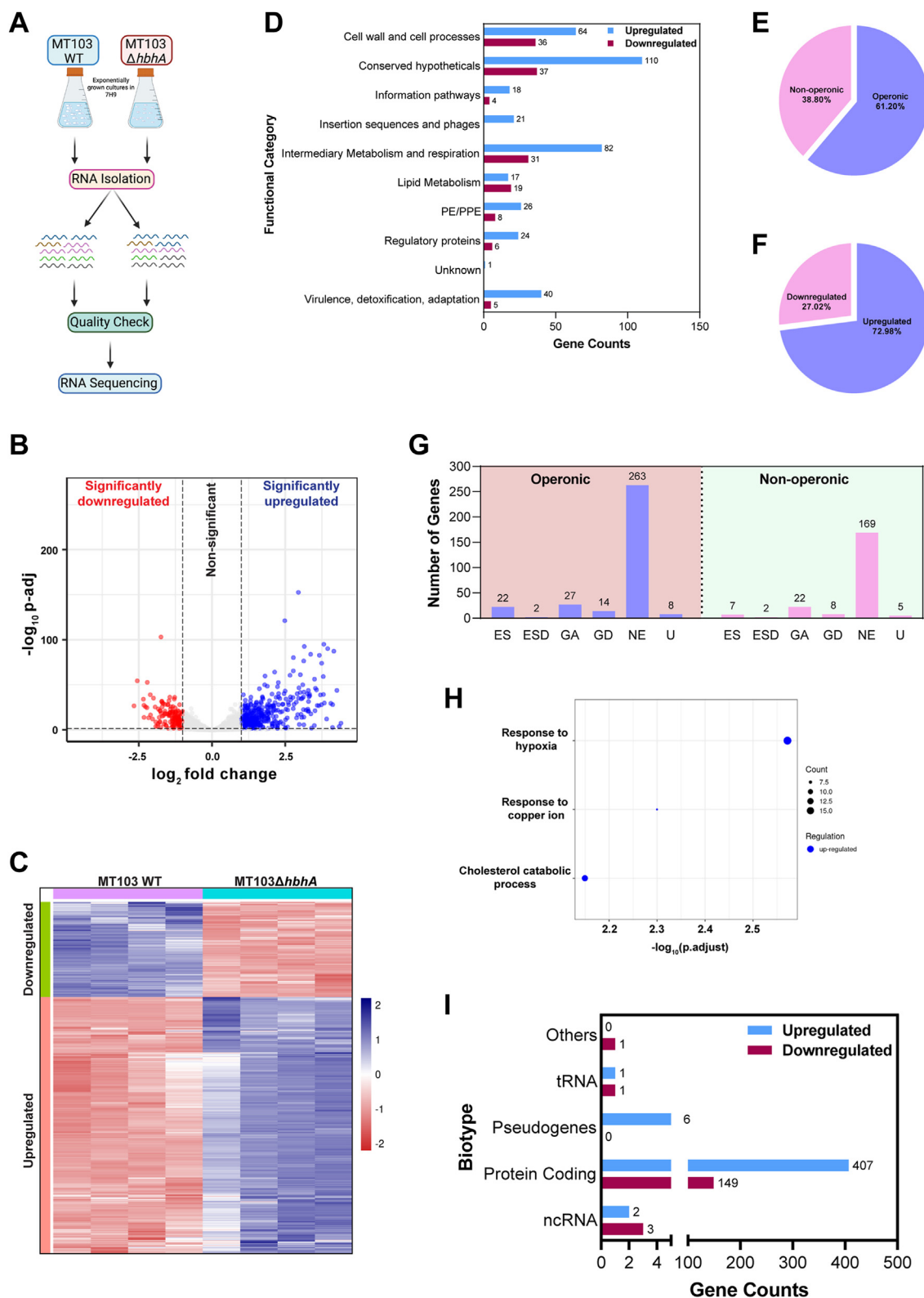


Figure 5. HbhA acts as a global transcriptional regulator. *A*, schematic representation of RNA-sequencing experiment. *B*, volcano plot showing the differentially expressed genes (DEGs) in *MT103ΔhbhA* in comparison to *MT103*. Red and blue dots denote significantly downregulated and upregulated genes upon applying a cutoff of \log_2 fold change > 1.0 and adjusted p -value < 0.05 . *C*, heatmaps showing the normalized read counts of all DEGs from four biological replicates of *MT103* and *MT103ΔhbhA*. Red and blue color intensities indicate relative downregulation and upregulation, respectively. *D*, bar graph showing the upregulated (blue) and downregulated (red) DEGs belonging to various functional categories. *E*, the pie chart depicting percentage of DEGs that are operonic and nonoperonic. *F*, the pie chart depicting the percentage of DEGs that are significantly upregulated and downregulated. *G*, bar graph depicting the number of operonic and nonoperonic DEGs belonging to essential (ES), essential domain (ESD), growth advantage (GA), growth defect (GD), nonessential (NE), and uncertain (U) categories. *H*, bubble plot depicting significantly enriched biological process categories of upregulated DEGs. *I*, bar graph depicting the number of significantly upregulated (blue) and downregulated (red) DEGs belonging to different biotypes. DEGs, differentially expressed genes; HbhA, heparin-binding hemagglutinin.

and Rv3852) (39, 40) are already well-characterized NAPs. The remaining two proteins RplV and HbhA were purified and their DNA binding ability was tested. RplV failed to bind to DNA in a gel shift assay (Fig. 1E). It is known to specifically bind to 23S rRNA (<https://mycobrowser.epfl.ch/genes/Rv0706>). On the other hand, HbhA showed efficient interaction with DNA. Therefore, further experiments were performed to understand the DNA-binding activities of HbhA and its role in the life cycle of *Mtb* as a NAP.

NAPs act as chromatin-architectural proteins because of their ability to interact with DNA at multiple places in a nonspecific manner (5). Although NAPs can bind to DNA in a sequence- and structure-independent manner, some of them prefer particular DNA sequences or structures. For example, H-NS from *E. coli* and *Salmonella* (71, 72), HupB, Lsr2, NapM, and NapA from *Mtb* (21, 24, 36, 41) show preferential binding to AT-rich DNA segments and downregulate the expression of horizontally acquired genes that are AT-rich (73). Similarly, several NAPs have a preferential binding affinity for different structures or forms of DNA. For example, CbpA from *E. coli* shows preferential binding for curved DNA (74), Lsr2 and HupB from *Mtb* show preferential binding to supercoiled DNA and cruciform DNA (Holliday junctions), respectively (29, 75). We observed highly efficient binding of HbhA to both supercoiled and linear forms of pUC19 DNA (Fig. 2, A and B), which led us to conclude that HbhA is a promiscuous DNA-binding protein.

A closer look at the primary structure of HbhA revealed the presence of a lysine-, alanine-, and proline-rich region in its carboxy-terminal domain, with five AKKA repeats (Fig. 1C). The C-terminal domain of HbhA was previously reported to associate with sulfated glycoconjugates present on the host epithelial cell membrane (76). Several other studies have linked the presence of lysine-, proline-, and alanine-rich repeats in histone H1/H5 with their DNA-binding ability (37, 38, 52). The HU homolog in *Mtb* possesses a highly basic extension containing multiple repeats of lysine-, alanine-, and proline-rich repeats in their C terminal end. The C-terminal region of HupB containing AKKA/PAKKA repeats is also responsible for the efficient binding of HupB to DNA (24). Our data indicate that the C-terminal domain harboring similar motifs is necessary and sufficient for the DNA-binding activity of HbhA (Fig. 2D).

Histones and other histone-like proteins or NAPs are known to protect DNA from damaging agents such as DNaseI (53) or hydroxyl radical cleavage (28), and act as the transcriptional regulators (56, 57, 77). HU homologs encoded by *Deinococcus radiodurans* protect the genome from several damaging agents like ionizing and UV radiations, and help survive the bacterium in extreme environmental conditions (78). Further, Lsr2, GroEL1, HupB, mIHF, NapM, and NapA from *Mtb* also protect DNA from DNaseI digestion and hydroxyl radical cleavage (21, 24, 28, 29, 36, 54, 55). We show that HbhA also protects DNA from DNaseI-mediated degradation (Fig. 3A). Lsr2, a functional homolog of H-NS in *Mtb*, acts as a repressor of the horizontally acquired genes (41) in addition to regulating the expression of genes involved in

physiology, antibiotic tolerance, and latency (27, 29). HU homologs are involved in the transcriptional regulation of genes involved in metabolism, general physiology, and virulence in case of *Salmonella* and *Francisella tularensis* (79, 80). The mycobacterial HU homolog, HupB regulates *katG* gene expression (26, 81), whose product is involved in activating isoniazid. Other mycobacterial NAPs such as mIHF, EspR, NapM, and NapA also regulate the expression of genes associated with general physiology, metabolism, and virulence (14, 21, 33, 36). We observed that HbhA acts as a transcriptional regulator since its binding inhibits transcription in an *in vitro* transcription assay (Fig. 3B).

NAPs protect DNA from damaging agents and act as global transcriptional regulators by modulating DNA topological and structural features. DNA supercoiling plays a major role in regulating gene expression and in maintaining the chromosomal architecture (82, 83). The introduction of negative supercoils in the DNA results in the opening of promoter regions and makes them accessible for RNA polymerase (84, 85). Further, NAPs such as Lsr2, HupB, and NapA regulate virulence-associated genes by inducing topological modulations in DNA in response to the environmental cues (21, 29, 75, 86, 87). We have observed that HbhA enhances topoisomerase I-mediated relaxation of DNA (Fig. 3C). Atomic force microscopic visualization of HbhA-DNA complexes revealed that HbhA also acts as a chromatin architectural protein since it introduces bends and loops in DNA (Fig. 3, D and E). NAPs are considered prokaryotic histone counterparts, as these proteins can induce structural changes in DNA by binding with it through various modes (bridging, bending, and wrapping) (5). For example, H-NS and its homologs from various bacterial species regulate gene expression and modulate bacterial chromosome architecture by bridging and coating the DNA (60, 88, 89).

The biochemical features of HbhA indicated that it could be a NAP. We also checked the localization of HbhA with the nucleoid of *Mtb* by isolating the nucleoids and detecting the presence of HbhA. We showed that HbhA is indeed associated with the nucleoid region of *Mtb* (Fig. 4, A and B), consistent with our hypothesis that HbhA is a NAP. Previous studies showed different localization patterns of HbhA. It was found to be present on the mycobacterial cell surface, secreted outside the mycobacterial cells and localized to the host cell mitochondria, and also present within the mycobacterial cells (90–92). HupB, a NAP of *Mtb*, and its homologs in *Mycobacterium smegmatis* and *Mycobacterium leprae* are also present on mycobacterial cell surface (93–95). HU, a highly conserved NAP throughout the prokaryotes, is detected on the bacterial cell surface and secreted outside the bacterial cell (96). In addition to prokaryotic NAPs, eukaryotic histones are also secreted in the extracellular milieu (97). However, the regulatory mechanisms behind multiple spatial localization of these proteins have not been elucidated.

HbhA deletion had no impact on the growth of *Mtb* in nutrient-rich 7H9 and nutrient-limiting Sauton's media (Fig. 4, D and E), suggesting that HbhA is a nonessential gene for *in vitro* survival of *Mtb* as reported earlier (32, 98, 99). While HbhA is

HbhA is a DNA-binding protein of *M. tuberculosis*

nonessential for the *in vivo* survival of *Mtb*, it is suggested to be involved in extrapulmonary dissemination because of its adhesion property with sulfated glycoconjugates present on the host epithelial cell membrane through its C-terminal domain (43). NAPs also tend to act as global transcriptional regulator (6). The HbhA regulon was examined by comparing the global transcriptional changes in the *hbhA* deleted strain to its parental counterpart. The transcriptomic study showed differential expression of ~36% of the total *Mtb* genes and ~29% of all essential genes ($\log_2fc > 0.5$ and $padj < 0.05$) (Table S3). These DEGs belong to multiple critical metabolic and virulence pathways such as virulence, detoxification, adaptation, cell wall synthesis and cell processes, lipid metabolism, and intermediary metabolism and respiration (Fig. 5D). ~73% of all DEGs showed upregulated expression upon *hbhA* deletion (Fig. 5E), suggesting HbhA as a plausible transcriptional repressor. Other *Mtb* NAPs, such as Lsr2 and mIHF, also regulate the expression of genes globally (27, 33, 41). Comparative analyses of the regulons of Lsr2 (27), mIHF (33), and HbhA showed that 35% and 4% of the HbhA regulon overlapped with the regulons of mIHF and Lsr2, respectively, and 5% of the HbhA regulon was shared by both mIHF and Lsr2 (Fig. S4, A and B and Table S4, B–D). This shows that HbhA is functionally similar to mIHF. The majority of DEGs of these NAPs belong mainly to cell wall and cell processes and intermediary metabolism and respiration (Fig. S4, C–F and Table S4, A–D).

In summary, we have characterized HbhA as a novel nucleoid-associated protein in *Mtb*, based on NAPs-like biochemical features such as DNA protection, transcriptional regulation, and topological and architectural modulations in DNA. The C-terminal domain of HbhA is the DNA-binding domain. Our results also showed that HbhA acts as a global transcriptional regulator. Even though deletion of *hbhA* influences the transcription of many essential genes, it is nonessential for *in vitro* growth in a complete medium. The transcriptional modulation observed of the essential genes may not be sufficient to display the eventual phenotypic impact on growth. The subsequent study can investigate the specific physiological relevance of the DNA-binding activity of HbhA.

Experimental procedures

Animal experimentation

All the animal experiment protocols were reviewed and approved by the Institutional Animal Ethics Committee of Department of Zoology, University of Delhi, India (the approved protocol number is DU/ZOOL/IAECR/2019). Balb/c mice were used for raising polyclonal antibodies used in the manuscript in accordance with the guidelines issued by the Committee for the Purpose of Control and Supervision of Experiments on Animals, Govt. of India.

Bacterial strains and growth conditions

E. coli DH5 α was used for cloning of the *Mtb* genes. For the expression of recombinant proteins, *E. coli* BL21 (Rossetta) was used as a surrogate host. *E. coli* cells were grown in LB broth at 37 °C, 200 rpm, and on LB agar medium at 37 °C (static

condition). Ampicillin and chloramphenicol were added at a final concentration of 100 μ g/ml, and 34 μ g/ml, respectively, wherever required. *Mtb* strains were grown in 7H9 Broth (Difco) supplemented with 0.85 g/L NaCl, 5 g/L BSA, 2 g/L dextrose, and 4 mg/L catalase (ADC), 0.2% glycerol, 0.05% Tween 80 at 37 °C, 200 rpm and on 7H10 Agar (Difco) supplemented with 0.85 g/L NaCl, 5 g/L BSA, 2 g/L dextrose, 4 mg/L catalase, and 50 mg/L oleic acid, 0.5% glycerol at 37 °C. Proper aeration (1:5 head space ratio) was maintained during the bacterial growth. Bacterial strains used or generated during this study are listed in Table 1.

Cloning, expression, and purification of recombinant proteins

Genes *rplV*, *lsr2*, *hbhA* (*rv0475*), *hbhA* Δ C (coding for the N-terminal fragment containing amino acids 1–160), *hbhA*_{151–199}, and *hbhA*_{161–199} (Coding for *hbhA* C-terminal domains, residues 151–199 and 161–199, respectively) were PCR amplified using the *Mtb* H37Rv genomic DNA as the template and primer pairs listed in Table 2. The amplicons were digested with respective restriction endonucleases and ligated into the corresponding sites of the previously digested expression vector pETPhos (Table 3).

For the expression of recombinant proteins, *E. coli* BL21 (Rossetta) containing the generated constructs were grown overnight and used as inoculum for 1 L cultures. Expression was induced at $A_{600} \sim 0.6$ using 1 mM IPTG at 37 °C for 3 h. Cells were pelleted and washed with PBS and stored at –80 °C until further processed. 6X-His-tagged recombinant proteins were purified as described previously (51, 100). Briefly, cells thawed on ice and resuspended in sonication buffer (50 mM Tris–Cl (pH 8.5), 300 mM NaCl, 10% glycerol, 20 mM imidazole, 1 mg/ml lysozyme, 1 mM PMSF, 1X protease inhibitor cocktail and 5 mM β -mercaptoethanol) and incubated on ice for 1 h with mild shaking. Cells were sonicated for nine pulses comprising 10 s on and 30 s off cycle. After sonication, the lysate was centrifuged at 16,000 rpm for 20 min, and the supernatant containing soluble recombinant protein was collected and loaded onto a Ni-NTA Superflow resin column, previously equilibrated with equilibration buffer A (50 mM Tris–Cl (pH 8.5), 300 mM NaCl, and 10% glycerol), buffer B (buffer A having 20 mM imidazole) and finally with 5 to 10 ml of sonication buffer. The column was washed with wash buffer A (50 mM Tris–Cl (pH 8.5), 300 mM NaCl, 10% glycerol, 20 mM imidazole, 1 mM PMSF, and 5 mM β -mercaptoethanol), wash buffer B (50 mM Tris–Cl (pH 8.5), 1 M NaCl, 10% glycerol, 20 mM imidazole, 1 mM PMSF, and 5 mM β -mercaptoethanol), again wash buffer A, and wash buffer C (50 mM Tris–Cl (pH 8.5), 300 mM NaCl, 10% glycerol, 50 mM imidazole, 1 mM PMSF, and 5 mM β -mercaptoethanol). Recombinant proteins were eluted with 50 mM Tris–Cl (pH 8.5), 150 mM NaCl, 10% glycerol, 200 mM imidazole. GST protein was purified as described (100). The purity of recombinant proteins was evaluated on 12% SDS-PAGE gel.

Electrophoretic mobility shift assay

DNA-protein interaction studies were performed using EMSAs as described previously (51), with slight modifications.

Table 1
List of bacterial strains used in this study

| Name | Genotype | Resistance Marker | Reference |
|---|---|--------------------------------|------------|
| DH5 α | <i>E. coli</i> F Φ 80 <i>lacZ</i> Δ M15 Δ (<i>lacZYA-argF</i>) U169 <i>recA1 endA1 hsdR17</i> (r _k ⁺ , m _k ⁻) <i>phoA supE44 thi-1 gyrA96 relA1</i> λ | - | Invitrogen |
| DH5 α -pETPhos | <i>E. coli</i> DH5 α strain producing pETPhos plasmid vector | Ampicillin | This study |
| DH5 α -pETPhos- <i>rplV</i> | <i>E. coli</i> DH5 α strain producing pETPhos- <i>rplV</i> plasmid | Ampicillin | This study |
| DH5 α -pETPhos- <i>hbhA</i> | <i>E. coli</i> DH5 α strain producing pETPhos- <i>hbhA</i> plasmid | Ampicillin | This study |
| DH5 α -pETPhos- <i>lsr2</i> | <i>E. coli</i> DH5 α strain producing pETPhos- <i>lsr2</i> plasmid | Ampicillin | This study |
| DH5 α -pETPhos- <i>rv0475</i> ₁₋₁₆₀ | <i>E. coli</i> DH5 α strain producing pETPhos- <i>rv0475</i> ₁₋₁₆₀ plasmid | Ampicillin | This study |
| DH5 α -pProExHTc | <i>E. coli</i> DH5 α strain producing pProExHTc plasmid vector | Ampicillin | This study |
| DH5 α -pProExHTc- <i>rv0475</i> ₁₅₁₋₁₉₉ | <i>E. coli</i> DH5 α strain producing pProExHTc- <i>rv0475</i> ₁₅₁₋₁₉₉ plasmid | Ampicillin | This study |
| DH5 α -pProExHTc- <i>rv0475</i> ₁₆₁₋₁₉₉ | <i>E. coli</i> DH5 α strain producing pProExHTc- <i>rv0475</i> ₁₆₁₋₁₉₉ plasmid | Ampicillin | This study |
| DH5 α -pGEX-5X3 | <i>E. coli</i> DH5 α strain producing pGEX-5X3 plasmid vector | Ampicillin | This study |
| DH5 α -pUC19 | <i>E. coli</i> DH5 α strain producing pUC19 plasmid vector | Ampicillin | This study |
| Rossetta (DE3) | <i>E. coli</i> F <i>ompT hsdS_B</i> (r _B ⁻ m _B ⁻) <i>gal dcm</i> (DE3) pRARE (Cam ^R) | Chloramphenicol | Merck |
| Rossetta (DE3)- pETPhos- <i>rplV</i> | <i>E. coli</i> Rossetta (DE3) strain having plasmid pETPhos- <i>rplV</i> | Ampicillin and chloramphenicol | This study |
| Rossetta (DE3)- pETPhos- <i>hbhA</i> | <i>E. coli</i> Rossetta (DE3) strain having plasmid pETPhos- <i>hbhA</i> | Ampicillin and chloramphenicol | This study |
| Rossetta (DE3)- pETPhos- <i>lsr2</i> | <i>E. coli</i> Rossetta (DE3) strain having plasmid pETPhos- <i>lsr2</i> | Ampicillin and chloramphenicol | This study |
| Rossetta (DE3)- pETPhos- <i>rv0475</i> ₁₋₁₆₀ | <i>E. coli</i> Rossetta (DE3) strain having plasmid pETPhos- <i>rv0475</i> ₁₋₁₆₀ | Ampicillin and chloramphenicol | This study |
| Rossetta (DE3)- pProExHTc- <i>rv0475</i> ₁₅₁₋₁₉₉ | <i>E. coli</i> Rossetta (DE3) strain having plasmid pProExHTc- <i>rv0475</i> ₁₅₁₋₁₉₉ | Ampicillin and chloramphenicol | This study |
| Rossetta (DE3)- pProExHTc- <i>rv0475</i> ₁₆₁₋₁₉₉ | <i>E. coli</i> Rossetta (DE3) strain having plasmid pProExHTc- <i>rv0475</i> ₁₆₁₋₁₉₉ | Ampicillin and chloramphenicol | This study |
| BL21(DE3) | <i>E. coli</i> B strain: F ⁻ <i>ompT gal dcm lon hsdS_B</i> (r _B ⁻ m _B ⁻) λ (DE3 [<i>lacI lacUV5-T7p07 ind1 sam7 nin5</i>]) [<i>malB</i> ⁺] _{K-12} (λ ^S) | - | Invitrogen |
| BL21(DE3)-pGEX-5X3 | <i>E. coli</i> BL21 (DE3) strain having plasmid pGEX-5X3 | Ampicillin | This study |
| H37Rv | WT <i>Mycobacterium tuberculosis</i> H37Rv strain | - | ATCC |
| MT103 | WT <i>Mycobacterium tuberculosis</i> 103 strain | - | (43) |
| MT103 Δ <i>hbhA</i> | <i>hbhA</i> deleted mutant of <i>Mycobacterium tuberculosis</i> 103 strain | Kanamycin | (43) |
| MT103 Δ <i>hbhA</i> :: <i>hbhA</i> | <i>hbhA</i> complemented strain of MT103 Δ <i>hbhA</i> | Kanamycin and hygromycin | (43) |

ATCC, American Type Culture Collection.

Briefly, for studying the interaction of proteins with nonspecific DNA template, pUC19 was used as a probe. DNA mixed with proteins at various DNA::protein molar ratios (1:0, 1:100, 1:250, 1:500, and 1:1000) were incubated at 25 °C for 30 min in a reaction buffer (10 mM Tris-Cl (pH 8.0), 50 mM NaCl, 50 μ g/ml bovine serum albumin (BSA), 1 mM DTT, 1 mM EDTA, and 5% glycerol) and resolved on 0.5% agarose gel using 1 \times Tris-borate-EDTA, running buffer. Ethidium bromide (EtBr) was used for visualization of native DNA and DNA-protein complexes.

DNaseI protection assay

DNaseI protection assays were carried out as described (24) with minor modifications. Briefly, 500 ng of pUC19 DNA was incubated with HbhA at molar ratios of 1:0, 1:250, 1:500, and

1:1000 (DNA::Protein) in the presence of a reaction buffer (100 mM Tris-Cl (pH 7.5), 25 mM MgCl₂, and 5 mM CaCl₂) at 25 °C for 30 min. An amount of 1 U of DNaseI (Invitrogen) was added, and the reaction was carried out at 37 °C for 30 s. The reactions were terminated by adding 1% SDS and 5 mM EDTA (final concentration), followed by electrophoresis on 1% agarose gel in 1X Tris-acetate-EDTA buffer. EtBr staining was used to visualize the DNA bands on the gel.

In vitro transcription assay

In vitro transcription assays were performed following the manufacturer's instruction (Riboprobe *in vitro* transcription assay kit, Promega) with slight modifications. Briefly, 250 ng of pGEM DNA was incubated with the various proteins at a molar ratio of 1:500 (DNA::Protein) for HbhA and HbhA Δ C in

Table 2
List of primers used in this study

| S.No. | Primers' name | Primers' sequence ^a (5'-3') |
|-------|-------------------------------|---|
| P1 | RplV FP ^b | GAACATATGACTGCGGCTACTAAGGCTACCG (NdeI) |
| P2 | RplV RP | CTTGGATCCCTAGTCTGAGCCTCCCTTCGCTGCAG (BamHI) |
| P3 | HbhA FP | GTTTCATATGGCTGAAAACCTCGAACATTGATG (NdeI) |
| P4 | HbhA RP | GATGGATCCCTACTTCTGGGTGACCTTCTTGGCC (BamHI) |
| P5 | Lsr2 FP | GAAACATATGGCGAAGAAAGTAACCGTCACC (NdeI) |
| P6 | Lsr2 RP | GATGCTAGCTCAGGTGCGCGCGTGGTATGCGTCCG (NheI) |
| P7 | HbhA Δ C RP | GGAGGATCCCTACTAGGCAGCTCGATGCCGACC (BamHI) |
| P8 | HbhA ₁₅₁₋₁₉₉ FP | CGCGGATCCGTCGCCCAAGCTGGTCCGCATCGAGC (BamHI) |
| P9 | HbhA ₁₆₁₋₁₉₉ FP | GCCGCCAAGCTGGTCCGGATCCCTAAGAAGGCTG (BamHI) |
| P10 | HbhA _{CTD} RP Common | GAGCCTCGAGCTACTTCTGGGTGACCTTCTTGGC (XhoI) |

^a Restriction sites are underlined and specified in the parentheses after the sequence.^b FP, Forward primer; RP, Reverse primer.

HbhA is a DNA-binding protein of *M. tuberculosis*

Table 3

List of plasmids used in this study

| Name | Description | Resistance marker | Reference |
|-------------------------------------|--|-------------------|------------|
| pETPhos | Plasmid used for recombinant protein expression in <i>E. coli</i> with N-terminal 6X-His tag | Ampicillin | Invitrogen |
| pETPhos-rplV | Expression of 6X-His-RplV in <i>E. coli</i> | Ampicillin | This study |
| pETPhos-hbhA | Expression of 6X-His-HbhA in <i>E. coli</i> | Ampicillin | This study |
| pETPhos-lsr2 | Expression of 6X-His-Lsr2 in <i>E. coli</i> | Ampicillin | This study |
| pETPhos-rv0475 ₁₋₁₆₀ | Expression of 6X-His-HbhA Δ C in <i>E. coli</i> | Ampicillin | This study |
| pProExHTc | Plasmid used for recombinant protein expression in <i>E. coli</i> with N-terminal 6X-His tag | Ampicillin | Invitrogen |
| pProExHTc-rv0475 ₁₅₁₋₁₉₉ | Expression of 6X-His-HbhA ₁₅₁₋₁₉₉ in <i>E. coli</i> | Ampicillin | This study |
| pProExHTc-rv0475 ₁₆₁₋₁₉₉ | Expression of 6X-His-HbhA ₁₆₁₋₁₉₉ in <i>E. coli</i> | Ampicillin | This study |
| pGEX-5X3 | Plasmid used for recombinant protein expression in <i>E. coli</i> with N-terminal GST tag | Ampicillin | Invitrogen |
| pUC19 | <i>E. coli</i> cloning vector | Ampicillin | Invitrogen |
| pGEM | Plasmid having T7 promoter used for <i>in-vitro</i> transcription assay | Ampicillin | Promega |

1X transcription buffer at 25 °C for 30 min. A total of 10 U of T7 RNA polymerase was added in a final reaction volume of 10 μ l and further incubated at 37 °C for 1 h. Reaction products were resolved using 1% agarose gel in 1X Tris-acetate-EDTA buffer and visualized by EtBr staining of the gel.

Topoisomerase I dependent DNA relaxation assay

Effect of HbhA on the supercoiling of plasmid DNA was studied according to the earlier described protocol (101). Briefly, 750 ng of pUC19 DNA was relaxed using 1 U *E. coli* Topoisomerase IA (New England Biolabs) in the presence of 1X CutSmart Buffer in a total reaction volume of 20 μ l at 37 °C for 1 h. Relaxed DNA was incubated with HbhA at a molar ratio of 1:1000 (DNA::Protein) at 25 °C for 30 min. Reactions were terminated by the addition of Proteinase K and incubation at 37 °C for 15 min. Samples were resolved in a 1% agarose gel in 1X Tris-borate-EDTA buffer and stained with EtBr for visualization.

Atomic force microscopy

Supercoiled or linear forms of pUC19 DNA were incubated for 30 min at 25 °C with each of the proteins (HbhA, HbhA Δ C, and Lsr2) at a molar ratio of 1:250. Ten microliters of the reaction mixture was loaded onto a freshly cleaved mica surface (Ted Pella, Inc). The unbound material was washed with filtered MilliQ water, and the mica was air dried. Images were acquired by using a 5500 scanning probe microscope (Keysight Technologies, Inc) and Keysight Technologies PicoView 1.20.3 software (<https://www.keysight.com/de/de/lib/software-detail/instrument-firmware-software/picoview-software/picoview-software-version-1-20-3.html#>) in tapping mode in air with 125- μ m-long silicon cantilevers (AppNano) with a resonance frequency of 200 to 400 kHz and a force constant of 13 to 77 N/m. The scan speed used was 1 line/s. Minimum image processing (first-order flattening and brightness contrast) was employed. Image analysis was performed using Pico Image Elements software v7.3 (<https://www.keysight.com/in/en/assets/7018-01697/data-sheets/5989-7596.pdf>).

Colocalization of HbhA with nucleoid of *Mtb*

To investigate the colocalization of HbhA with nucleoids of *Mtb*; nucleoids were isolated by sucrose-density gradient centrifugation as described (54). Briefly, glycine was added at a final concentration of 1% to exponentially growing cultures

and incubated for 2 h at 37 °C and 200 rpm. Cells were harvested, washed with PBS (pH 7.4), resuspended in 5 ml chilled acetone and incubated at -20 °C for 1 h. Cells were harvested, air dried, resuspended in 1 ml extraction buffer containing 20% sucrose, 1 mg/ml lysozyme, and 1X Protease Inhibitor cocktail (Roche), and incubated overnight at 37 °C and 200 rpm. Finally, 1% of NP-40 was added to the mixture, incubated for 2 h at 37 °C and 200 rpm, and centrifuged at 3000g to remove the debris. Lysates containing nucleoids were passed through a 0.22 μ m filter. Cleared lysates were layered onto a 12 to 60% sucrose density gradient and was centrifuged at 4000g and 4 °C for 15 min in a swing bucket rotor. The tube's bottom was punctured to collect sucrose gradient fractions of 500 μ l each. The presence of DNA in the fractions was measured at $A_{260\text{ nm}}$, and the amount of DNA was plotted against the fraction numbers. The fractions containing the highest amount of DNA were considered nucleoid-containing fractions.

The *Mtb* nucleoid fractions were resolved using a 12% SDS-PAGE and transferred onto the nitrocellulose membrane. The presence of HbhA with nucleoid region was detected using antibodies by immunoblotting.

Immunoblotting

For immunoblotting, nucleoid fractions containing 40 μ g proteins were separated on 12% SDS-PAGE and transferred to nitrocellulose membranes (Millipore). After blocking with 3% BSA in PBS containing 0.05% Tween 20 (PBST) for 1 h, membranes were washed three times with PBST and incubated overnight with primary antibodies anti-His-HbhA (1:5000) or anti-His-GroEL2 (1:10,000) antibodies at 4 °C. These antibodies were generated in mice using purified recombinant proteins as antigens. One percent of BSA was added to prevent nonspecific antibody binding. Membranes were washed five times with PBST and treated with anti-mouse immunoglobulin G antibody conjugated to horseradish peroxidase (1:10,000-Cell Signaling Technology, Cat. No. 7076S) for an hour. Membranes were washed again with PBST five times and finally developed using SuperSignal West Pico PLUS/Femto chemiluminescent substrate (Thermo Fisher Scientific).

Growth kinetics, RNA isolation, and transcriptomics

Exponentially grown *Mtb* cultures (*MT103*, *MT103 Δ hbhA*, and *MT103 Δ hbhA::hbhA*) in the 7H9-ADC medium were inoculated at an initial $A_{600\text{ nm}}$ of 0.05 in

nutrient-rich 7H9 or nutrient-limited Sauton's media and allowed to grow at 37 °C, 200 rpm. Growth kinetics was monitored by measuring A_{600} every 24 h, and serial dilutions of cultures were plated on 7H11 agar plates for colony-forming units enumeration.

RNA was isolated using TRIzol reagent (Ambion). Cell numbers equivalent to A_{600} of 10 of exponentially grown *MT103* and *MT103ΔhbhA* strains were harvested by centrifugation and resuspended in TRIzol reagent. Following cell lysis using 0.1 mm zirconium beads, RNA was extracted with chloroform, precipitated with isopropanol, and washed with 75% ethanol. RNA pellets were air dried and dissolved in nuclease free water (102). Isolated RNA was subjected to DNaseI treatment to remove DNA contamination from the samples.

RNA isolated from four independent biological replicates were used for RNA-sequencing and transcriptomics analyses as per the earlier described protocol (102). Sequencing was performed at the core sequencing facility of the Centre for Cellular and Molecular Biology, Hyderabad, India.

Functional enrichment analysis

DAVID web services (<https://david.ncifcrf.gov>) were used for functional enrichment analysis. Only GO terms and KEGG pathways were selected for gene enrichment analysis.

Statistical analysis

Data reproducibility was ensured by performing experiments in three independent biological replicates, unless stated otherwise. Data plotting and statistical significance calculation were performed using GraphPad Prism software (Prism 9) (<https://www.graphpad.com/features>). Two-way ANOVA followed by a post hoc Tukey's test was employed to analyze statistical significance.

Figures preparation

Bio Render was used to prepare illustrations/schematics, whereas ImageJ and Adobe Illustrator were used to prepare scientific figures.

Data availability

RNA-seq data are available at the NCBI Gene Expression Omnibus Database with accession number GSE235293 (<https://www.ncbi.nlm.nih.gov/geo/query/acc.cgi?acc=GSE235293>).

Supporting information—This article contains supporting information.

Acknowledgments—We thank the core sequencing facility of CSIR-CCMB, Hyderabad. We thank Dr Ramandeep Singh and his student Dr Amardeep, Translational Health Science and Technology Institute, Faridabad, for their help while cloning the *hbhA* and *rplV* gene. We would also like to thank Dr Anurag Agrawal, and Dr Sagarika Biswas, CSIR-Institute of Genomics and Integrative Biology, Delhi, for their support and for providing the required facilities. We also acknowledge the BSL3 facility at the University

of Delhi South Campus and National Institute of Immunology for extending their facility usage.

Author contributions—C. C. K., M. Gupta, V. K. N., and Y. S. conceptualization; C. C. K., S. N., A. Gupta, P. S., M. K., D. T. S., M. Gupta, V. K. N., and Y. S. methodology; C. C. K., S. N., A. Gupta, P. S., M. K., A. Gangwal, E. T., S. G., N. K. S., and D. T. S. investigation; C. C. K., M. Gupta, V. K. N., and Y. S. validation; C. C. K., N. S., N. K., N. K. S., and D. T. S. formal analysis; C. C. K. data curation; C. C. K. writing—original draft; C. C. K., S. N., A. Gupta, P. S., M. K., A. Gangwal, N. S., N. K., E. T., S. G., N. K. S., D. T. S., G. K., M. Ganguli, D. R., C. L., S. B. M., M. Gupta, V. K. N., and Y. S. writing—review and editing; D. T. S., S. B. M., M. Gupta, V. K. N., and Y. S. supervision; G. K., M. Ganguly, D. R., C. L., V. K. N., and Y. S. resources; M. Gupta, V. K. N., and Y. S. project administration; V. K. N. and Y. S. funding acquisition.

Funding and additional information—We acknowledge support from J C Bose fellowship (SERB) to Y. S. and V. K. N. C. C. K., A. G., and N. K. are supported by University Grant Commission (UGC), N. S. and E. T. are supported by Council of Scientific and Industrial Research (CSIR), and M. Gupta is supported by CSIR (SRA).

Conflict of interest—The authors declare that they have no conflicts of interest with the contents of this article.

Abbreviations—The abbreviations used are: BSA, bovine serum albumin; DEGs, differentially expressed genes; EtBr, ethidium bromide; HbhA, heparin-binding hemagglutinin; mIHF, mycobacterial integration host factor; *Mtb*, *Mycobacterium tuberculosis*; NAPs, nucleoid-associated proteins; PBST, PBS containing 0.05% Tween 20.

References

1. Toro, E., and Shapiro, L. (2010) Bacterial chromosome organization and segregation. *Cold Spring Harb. Perspect. Biol.* **2**, a000349
2. Wang, X., Montero Llopis, P., and Rudner, D. Z. (2014) *Bacillus subtilis* chromosome organization oscillates between two distinct patterns. *Proc. Natl. Acad. Sci. U. S. A.* **111**, 12877–12882
3. Niki, H., Yamaichi, Y., and Hiraga, S. (2000) Dynamic organization of chromosomal DNA in *Escherichia coli*. *Genes Dev.* **14**, 212–223
4. Bates, D., and Kleckner, N. (2005) Chromosome and replisome dynamics in *E. coli*: loss of sister cohesion triggers global chromosome movement and mediates chromosome segregation. *Cell* **121**, 899–911
5. Luijsterburg, M. S., Noom, M. C., Wuite, G. J., and Dame, R. T. (2006) The architectural role of nucleoid-associated proteins in the organization of bacterial chromatin: a molecular perspective. *J. Struct. Biol.* **156**, 262–272
6. Dillon, S. C., and Dorman, C. J. (2010) Bacterial nucleoid-associated proteins, nucleoid structure and gene expression. *Nat. Rev. Microbiol.* **8**, 185–195
7. Wang, W., Li, G. W., Chen, C., Xie, X. S., and Zhuang, X. (2011) Chromosome organization by a nucleoid-associated protein in live bacteria. *Science* **333**, 1445–1449
8. Badrinarayanan, A., Le, T. B., and Laub, M. T. (2015) Bacterial chromosome organization and segregation. *Annu. Rev. Cell Dev. Biol.* **31**, 171–199
9. Ali Azam, T., Iwata, A., Nishimura, A., Ueda, S., and Ishihama, A. (1999) Growth phase-dependent variation in protein composition of the *Escherichia coli* nucleoid. *J. Bacteriol.* **181**, 6361–6370
10. Postow, L., Hardy, C. D., Arsuaga, J., and Cozzarelli, N. R. (2004) Topological domain structure of the *Escherichia coli* chromosome. *Genes Dev.* **18**, 1766–1779

HbhA is a DNA-binding protein of *M. tuberculosis*

11. Stavans, J., and Oppenheim, A. (2006) DNA-protein interactions and bacterial chromosome architecture. *Phys. Biol.* **3**, R1–10
12. Kahramanoglu, C., Seshasayee, A. S., Prieto, A. I., Ibberson, D., Schmidt, S., Zimmermann, J., et al. (2011) Direct and indirect effects of H-NS and Fis on global gene expression control in *Escherichia coli*. *Nucleic Acids Res.* **39**, 2073–2091
13. Berger, M., Farcas, A., Geertz, M., Zhelyazkova, P., Brix, K., Travers, A., et al. (2010) Coordination of genomic structure and transcription by the main bacterial nucleoid-associated protein HU. *EMBO Rep.* **11**, 59–64
14. Blasco, B., Chen, J. M., Hartkoorn, R., Sala, C., Uplekar, S., Rougemont, J., et al. (2012) Virulence regulator EspR of *Mycobacterium tuberculosis* is a nucleoid-associated protein. *PLoS Pathog.* **8**, e1002621
15. Chodavarapu, S., Felczak, M. M., Yaniv, J. R., and Kaguni, J. M. (2008) *Escherichia coli* DnaA interacts with HU in initiation at the *E. coli* replication origin. *Mol. Microbiol.* **67**, 781–792
16. Kasho, K., Fujimitsu, K., Matoba, T., Oshima, T., and Katayama, T. (2014) Timely binding of IHF and Fis to DARS2 regulates ATP-DnaA production and replication initiation. *Nucleic Acids Res.* **42**, 13134–13149
17. Kamashev, D., and Rouviere-Yaniv, J. (2000) The histone-like protein HU binds specifically to DNA recombination and repair intermediates. *EMBO J.* **19**, 6527–6535
18. Lee, C., and Marians, K. J. (2013) Characterization of the nucleoid-associated protein YejK. *J. Biol. Chem.* **288**, 31503–31516
19. Teramoto, J., Yoshimura, S. H., Takeyasu, K., and Ishihama, A. (2010) A novel nucleoid protein of *Escherichia coli* induced under anaerobic growth conditions. *Nucleic Acids Res.* **38**, 3605–3618
20. Azam, T. A., and Ishihama, A. (1999) Twelve species of the nucleoid-associated protein from *Escherichia coli*. Sequence recognition specificity and DNA binding affinity. *J. Biol. Chem.* **274**, 33105–33113
21. Datta, C., Jha, R. K., Ganguly, S., and Nagaraja, V. (2019) NapA (Rv0430), a novel nucleoid-associated protein that regulates a virulence operon in *Mycobacterium tuberculosis* in a supercoiling-dependent manner. *J. Mol. Biol.* **431**, 1576–1591
22. Kriel, N. L., Gallant, J., van Wyk, N., van Helden, P., Sampson, S. L., Warren, R. M., et al. (2018) Mycobacterial nucleoid associated proteins: an added dimension in gene regulation. *Tuberculosis (Edinb)* **108**, 169–177
23. Pandey, S. D., Choudhury, M., Yousuf, S., Wheeler, P. R., Gordon, S. V., Ranjan, A., et al. (2014) Iron-regulated protein HupB of *Mycobacterium tuberculosis* positively regulates siderophore biosynthesis and is essential for growth in macrophages. *J. Bacteriol.* **196**, 1853–1865
24. Kumar, S., Sardesai, A. A., Basu, D., Muniyappa, K., and Hasnain, S. E. (2010) DNA clasp by mycobacterial HU: the C-terminal region of HupB mediates increased specificity of DNA binding. *PLoS One* **5**, e12551
25. Mukherjee, A., Bhattacharyya, G., and Grove, A. (2008) The C-terminal domain of HU-related histone-like protein Hlp from *Mycobacterium smegmatis* mediates DNA end-joining. *Biochemistry* **47**, 8744–8753
26. Niki, M., Niki, M., Tateishi, Y., Ozeki, Y., Kirikae, T., Lewin, A., et al. (2012) A novel mechanism of growth phase-dependent tolerance to isoniazid in mycobacteria. *J. Biol. Chem.* **287**, 27743–27752
27. Bartek, I. L., Woolhiser, L. K., Baughn, A. D., Basaraba, R. J., Jacobs, W. R., Jr., Lenaerts, A. J., et al. (2014) Mycobacterium tuberculosis Lsr2 is a global transcriptional regulator required for adaptation to changing oxygen levels and virulence. *mBio* **5**, e01106-14
28. Colangeli, R., Haq, A., Arcus, V. L., Summers, E., Magliozzo, R. S., McBride, A., et al. (2009) The multifunctional histone-like protein Lsr2 protects mycobacteria against reactive oxygen intermediates. *Proc. Natl. Acad. Sci. U. S. A.* **106**, 4414–4418
29. Colangeli, R., Helb, D., Vilcheze, C., Hazbon, M. H., Lee, C. G., Safi, H., et al. (2007) Transcriptional regulation of multi-drug tolerance and antibiotic-induced responses by the histone-like protein Lsr2 in *M. tuberculosis*. *PLoS Pathog.* **3**, e87
30. Chen, J. M., German, G. J., Alexander, D. C., Ren, H., Tan, T., and Liu, J. (2006) Roles of Lsr2 in colony morphology and biofilm formation of *Mycobacterium smegmatis*. *J. Bacteriol.* **188**, 633–641
31. Raghavan, S., Manzanillo, P., Chan, K., Dovey, C., and Cox, J. S. (2008) Secreted transcription factor controls *Mycobacterium tuberculosis* virulence. *Nature* **454**, 717–721
32. Griffin, J. E., Gawronski, J. D., Dejesus, M. A., Ioerger, T. R., Akerley, B. J., and Sasseti, C. M. (2011) High-resolution phenotypic profiling defines genes essential for mycobacterial growth and cholesterol catabolism. *PLoS Pathog.* **7**, e1002251
33. Odermatt, N. T., Sala, C., Benjak, A., and Cole, S. T. (2018) Essential nucleoid associated protein mIHF (Rv1388) controls virulence and housekeeping genes in *Mycobacterium tuberculosis*. *Sci. Rep.* **8**, 14214
34. Schubert, O. T., Mouritsen, J., Ludwig, C., Rost, H. L., Rosenberger, G., Arthur, P. K., et al. (2013) The Mtb proteome library: a resource of assays to quantify the complete proteome of *Mycobacterium tuberculosis*. *Cell Host Microbe* **13**, 602–612
35. Liu, Y., Xie, Z., Zhou, X., Li, W., Zhang, H., and He, Z. G. (2019) NapM enhances the survival of *Mycobacterium tuberculosis* under stress and in macrophages. *Commun. Biol.* **2**, 65
36. Liu, Y., Wang, H., Cui, T., Zhou, X., Jia, Y., Zhang, H., et al. (2016) NapM, a new nucleoid-associated protein, broadly regulates gene expression and affects mycobacterial resistance to anti-tuberculosis drugs. *Mol. Microbiol.* **101**, 167–181
37. Khadake, J. R., and Rao, M. R. (1995) DNA- and chromatin-condensing properties of rat testes H1a and H1t compared to those of rat liver H1bdec; H1t is a poor condenser of chromatin. *Biochemistry* **34**, 15792–15801
38. Churchill, M. E., and Travers, A. A. (1991) Protein motifs that recognize structural features of DNA. *Trends Biochem. Sci.* **16**, 92–97
39. Prabhakar, S., Annapurna, P. S., Jain, N. K., Dey, A. B., Tyagi, J. S., and Prasad, H. K. (1998) Identification of an immunogenic histone-like protein (HLPmt) of *Mycobacterium tuberculosis*. *Tuber Lung Dis.* **79**, 43–53
40. Werlang, I. C. R., Schneider, C. Z., Mendonca, J. D., Palma, M. S., Basso, L. A., and Santos, D. S. (2009) Identification of Rv3852 as a nucleoid-associated protein in *Mycobacterium tuberculosis*. *Microbiology (Reading)* **155**, 2652–2663
41. Gordon, B. R., Li, Y., Wang, L., Sintsova, A., van Bakel, H., Tian, S., et al. (2010) Lsr2 is a nucleoid-associated protein that targets AT-rich sequences and virulence genes in *Mycobacterium tuberculosis*. *Proc. Natl. Acad. Sci. U. S. A.* **107**, 5154–5159
42. Menozzi, F. D., Bischoff, R., Fort, E., Brennan, M. J., and Loch, C. (1998) Molecular characterization of the mycobacterial heparin-binding hemagglutinin, a mycobacterial adhesin. *Proc. Natl. Acad. Sci. U. S. A.* **95**, 12625–12630
43. Pethe, K., Alonso, S., Biet, F., Delogu, G., Brennan, M. J., Loch, C., et al. (2001) The heparin-binding haemagglutinin of *M. tuberculosis* is required for extrapulmonary dissemination. *Nature* **412**, 190–194
44. Grasser, K. D., Ritt, C., Krieg, M., Fernandez, S., Alonso, J. C., and Grimm, R. (1997) The recombinant product of the *Chrytomonas phi* plastid gene hlpA is an architectural HU-like protein that promotes the assembly of complex nucleoprotein structures. *Eur. J. Biochem.* **249**, 70–76
45. Kamau, E., Tshilis, N. D., Simmons, L. A., and Grove, A. (2005) Surface salt bridges modulate the DNA site size of bacterial histone-like HU proteins. *Biochem. J.* **390**, 49–55
46. Delogu, G., and Brennan, M. J. (1999) Functional domains present in the mycobacterial hemagglutinin, HBHA. *J. Bacteriol.* **181**, 7464–7469
47. Esposito, C., Carullo, P., Pedone, E., Graziano, G., Del Vecchio, P., and Berisio, R. (2010) Dimerisation and structural integrity of Heparin Binding Hemagglutinin A from *Mycobacterium tuberculosis*: implications for bacterial agglutination. *FEBS Lett.* **584**, 1091–1096
48. Squeglia, F., Ruggiero, A., De Simone, A., and Berisio, R. (2018) A structural overview of mycobacterial adhesins: key biomarkers for diagnostics and therapeutics. *Protein Sci.* **27**, 369–380
49. Paci, M., Pon, C. L., Losso, M. A., and Gualerzi, C. (1984) Proteins from the prokaryotic nucleoid. High-resolution 1H NMR spectroscopic study

- of *Escherichia coli* DNA-binding proteins NS1 and NS2. *Eur. J. Biochem.* **138**, 193–200
50. Suzuki, M. (1989) SPKK, a new nucleic acid-binding unit of protein found in histone. *EMBO J.* **8**, 797–804
 51. Gupta, M., Sajid, A., Sharma, K., Ghosh, S., Arora, G., Singh, R., *et al.* (2014) HupB, a nucleoid-associated protein of *Mycobacterium tuberculosis*, is modified by serine/threonine protein kinases *in vivo*. *J. Bacteriol.* **196**, 2646–2657
 52. Khadake, J. R., and Rao, M. R. (1997) Condensation of DNA and chromatin by an SPKK-containing octapeptide repeat motif present in the C-terminus of histone H1. *Biochemistry* **36**, 1041–1051
 53. Grayling, R. A., Bailey, K. A., and Reeve, J. N. (1997) DNA binding and nuclease protection by the Hmf histones from the hyperthermophilic archaeon *Methanothermus fervidus*. *Extremophiles* **1**, 79–88
 54. Basu, D., Khare, G., Singh, S., Tyagi, A., Khosla, S., and Mande, S. C. (2009) A novel nucleoid-associated protein of *Mycobacterium tuberculosis* is a sequence homolog of GroEL. *Nucleic Acids Res.* **37**, 4944–4954
 55. Mishra, A., Vij, M., Kumar, D., Taneja, V., Mondal, A. K., Bothra, A., *et al.* (2013) Integration host factor of *Mycobacterium tuberculosis*, mIHF, compacts DNA by a bending mechanism. *PLoS One* **8**, e69985
 56. Yang, J., Camakaris, H., and Pittard, A. J. (1996) *In vitro* transcriptional analysis of TyrR-mediated activation of the mtr and tyrP+3 promoters of *Escherichia coli*. *J. Bacteriol.* **178**, 6389–6393
 57. van Ulsen, P., Hillebrand, M., Zuilianello, L., van de Putte, P., and Goosen, N. (1996) Integration host factor alleviates the H-NS-mediated repression of the early promoter of bacteriophage Mu. *Mol. Microbiol.* **21**, 567–578
 58. Rimsky, S. (2004) Structure of the histone-like protein H-NS and its role in regulation and genome superstructure. *Curr. Opin. Microbiol.* **7**, 109–114
 59. Swiercz, J. P., Nanji, T., Gloyd, M., Guarne, A., and Elliot, M. A. (2013) A novel nucleoid-associated protein specific to the actinobacteria. *Nucleic Acids Res.* **41**, 4171–4184
 60. Chen, J. M., Ren, H., Shaw, J. E., Wang, Y. J., Li, M., Leung, A. S., *et al.* (2008) Lsr2 of *Mycobacterium tuberculosis* is a DNA-bridging protein. *Nucleic Acids Res.* **36**, 2123–2135
 61. Anderson, C. J., and Kendall, M. M. (2017) *Salmonella enterica* serovar typhimurium strategies for host adaptation. *Front. Microbiol.* **8**, 1983
 62. Singh, S. K. (2017) *Staphylococcus aureus* intracellular survival: a closer look in the process. *Virulence* **8**, 1506–1507
 63. Bussi, C., and Gutierrez, M. G. (2019) *Mycobacterium tuberculosis* infection of host cells in space and time. *FEMS Microbiol. Rev.* **43**, 341–361
 64. Boor, K. J. (2006) Bacterial stress responses: what doesn't kill them can make them stronger. *PLoS Biol.* **4**, e23
 65. Morikawa, K., Ohniwa, R. L., Kim, J., Maruyama, A., Ohta, T., and Takeyasu, K. (2006) Bacterial nucleoid dynamics: oxidative stress response in *Staphylococcus aureus*. *Genes Cells* **11**, 409–423
 66. Trojanowski, D., Kolodziej, M., Holowka, J., Muller, R., and Zakrzewska-Czerwinska, J. (2019) Watching DNA replication inhibitors in action: exploiting time-lapse microfluidic microscopy as a tool for target-drug interaction studies in *Mycobacterium*. *Antimicrob. Agents Chemother.* **63**, e00739-19
 67. de Vries, R. (2010) DNA condensation in bacteria: interplay between macromolecular crowding and nucleoid proteins. *Biochimie* **92**, 1715–1721
 68. Jeon, C., Jung, Y., and Ha, B. Y. (2017) A ring-polymer model shows how macromolecular crowding controls chromosome-arm organization in *Escherichia coli*. *Sci. Rep.* **7**, 11896
 69. Joyeux, M. (2019) Preferential localization of the bacterial nucleoid. *Microorganisms* **7**, 204
 70. Holowka, J., and Zakrzewska-Czerwinska, J. (2020) Nucleoid associated proteins: the small organizers that help to cope with stress. *Front. Microbiol.* **11**, 590
 71. Navarre, W. W., Porwollik, S., Wang, Y., McClelland, M., Rosen, H., Libby, S. J., *et al.* (2006) Selective silencing of foreign DNA with low GC content by the H-NS protein in *Salmonella*. *Science* **313**, 236–238
 72. Lucchini, S., Rowley, G., Goldberg, M. D., Hurd, D., Harrison, M., and Hinton, J. C. (2006) H-NS mediates the silencing of laterally acquired genes in bacteria. *PLoS Pathog.* **2**, e81
 73. Ali, S. S., Xia, B., Liu, J., and Navarre, W. W. (2012) Silencing of foreign DNA in bacteria. *Curr. Opin. Microbiol.* **15**, 175–181
 74. Ueguchi, C., Kakeda, M., Yamada, H., and Mizuno, T. (1994) An analogue of the DnaJ molecular chaperone in *Escherichia coli*. *Proc. Natl. Acad. Sci. U. S. A.* **91**, 1054–1058
 75. Sharadamma, N., Khan, K., Kumar, S., Patil, K. N., Hasnain, S. E., and Muniyappa, K. (2011) Synergy between the N-terminal and C-terminal domains of *Mycobacterium tuberculosis* HupB is essential for high-affinity binding, DNA supercoiling and inhibition of RecA-promoted strand exchange. *FEBS J.* **278**, 3447–3462
 76. Delogu, G., Fadda, G., and Brennan, M. J. (2012) Impact of structural domains of the heparin binding hemagglutinin of *Mycobacterium tuberculosis* on function. *Protein Pept. Lett.* **19**, 1035–1039
 77. Shahul Hameed, U. F., Liao, C., Radhakrishnan, A. K., Huser, F., Aljedani, S. S., Zhao, X., *et al.* (2019) H-NS uses an autoinhibitory conformational switch for environment-controlled gene silencing. *Nucleic Acids Res.* **47**, 2666–2680
 78. Nguyen, H. H., de la Tour, C. B., Toueille, M., Vannier, F., Sommer, S., and Servant, P. (2009) The essential histone-like protein HU plays a major role in *Deinococcus radiodurans* nucleoid compaction. *Mol. Microbiol.* **73**, 240–252
 79. Mangan, M. W., Lucchini, S., T. O. C., Fitzgerald, S., Hinton, J. C. D., and Dorman, C. J. (2011) Nucleoid-associated protein HU controls three regulons that coordinate virulence, response to stress and general physiology in *Salmonella enterica* serovar Typhimurium. *Microbiology (Reading)* **157**, 1075–1087
 80. Stojkova, P., Spidlova, P., Lenco, J., Rehulkova, H., Kratka, L., and Stulik, J. (2018) HU protein is involved in intracellular growth and full virulence of *Francisella tularensis*. *Virulence* **9**, 754–770
 81. Enany, S., Yoshida, Y., Tateishi, Y., Ozeki, Y., Nishiyama, A., Savitskaya, A., *et al.* (2017) *Mycobacterial* DNA-binding protein 1 is critical for long term survival of *Mycobacterium smegmatis* and simultaneously coordinates cellular functions. *Sci. Rep.* **7**, 6810
 82. Dorman, C. J., and Ni Bhriain, N. (1993) DNA topology and bacterial virulence gene regulation. *Trends Microbiol.* **1**, 92–99
 83. Dorman, C. J. (2006) DNA supercoiling and bacterial gene expression. *Sci. Prog.* **89**, 151–166
 84. Muskhelishvili, G., Buckle, M., Heumann, H., Kahmann, R., and Travers, A. A. (1997) FIS activates sequential steps during transcription initiation at a stable RNA promoter. *EMBO J.* **16**, 3655–3665
 85. Travers, A., and Muskhelishvili, G. (1998) DNA microloops and microdomains: a general mechanism for transcription activation by torsional transmission. *J. Mol. Biol.* **279**, 1027–1043
 86. Dorman, C. J. (2013) Co-operative roles for DNA supercoiling and nucleoid-associated proteins in the regulation of bacterial transcription. *Biochem. Soc. Trans.* **41**, 542–547
 87. Ghosh, S., Mallick, B., and Nagaraja, V. (2014) Direct regulation of topoisomerase activity by a nucleoid-associated protein. *Nucleic Acids Res.* **42**, 11156–11165
 88. Dame, R. T., Luijsterburg, M. S., Krin, E., Bertin, P. N., Wagner, R., and Wuite, G. J. (2005) DNA bridging: a property shared among H-NS-like proteins. *J. Bacteriol.* **187**, 1845–1848
 89. Kotlajich, M. V., Hron, D. R., Boudreau, B. A., Sun, Z., Lyubchenko, Y. L., and Landick, R. (2015) Bridged filaments of histone-like nucleoid structuring protein pause RNA polymerase and aid termination in bacteria. *Elife* **4**, e04970
 90. Menozzi, F. D., Rouse, J. H., Alavi, M., Laude-Sharp, M., Muller, J., Bischoff, R., *et al.* (1996) Identification of a heparin-binding hemagglutinin present in mycobacteria. *J. Exp. Med.* **184**, 993–1001

HbhA is a DNA-binding protein of *M. tuberculosis*

91. Raze, D., Verwaerde, C., Deloison, G., Werkmeister, E., Coupin, B., Loyens, M., *et al.* (2018) Heparin-binding hemagglutinin adhesin (HBHA) is involved in intracytosolic lipid inclusions formation in mycobacteria. *Front. Microbiol.* **9**, 2258
92. Sohn, H., Kim, J. S., Shin, S. J., Kim, K., Won, C. J., Kim, W. S., *et al.* (2011) Targeting of Mycobacterium tuberculosis heparin-binding hemagglutinin to mitochondria in macrophages. *PLoS Pathog.* **7**, e1002435
93. Pethe, K., Puech, V., Daffe, M., Josenhans, C., Drobecq, H., Locht, C., *et al.* (2001) Mycobacterium smegmatis laminin-binding glycoprotein shares epitopes with Mycobacterium tuberculosis heparin-binding haemagglutinin. *Mol. Microbiol.* **39**, 89–99
94. Shimoji, Y., Ng, V., Matsumura, K., Fischetti, V. A., and Rambukkana, A. (1999) A 21-kDa surface protein of Mycobacterium leprae binds peripheral nerve laminin-2 and mediates Schwann cell invasion. *Proc. Natl. Acad. Sci. U. S. A.* **96**, 9857–9862
95. Aoki, K., Matsumoto, S., Hirayama, Y., Wada, T., Ozeki, Y., Niki, M., *et al.* (2004) Extracellular mycobacterial DNA-binding protein 1 participates in mycobacterium-lung epithelial cell interaction through hyaluronic acid. *J. Biol. Chem.* **279**, 39798–39806
96. Stojkova, P., and Spidlova, P. (2022) Bacterial nucleoid-associated protein HU as an extracellular player in host-pathogen interaction. *Front. Cell Infect. Microbiol.* **12**, 999737
97. Chen, R., Kang, R., Fan, X. G., and Tang, D. (2014) Release and activity of histone in diseases. *Cell Death Dis.* **5**, e1370
98. Sassetti, C. M., Boyd, D. H., and Rubin, E. J. (2003) Genes required for mycobacterial growth defined by high density mutagenesis. *Mol. Microbiol.* **48**, 77–84
99. Minato, Y., Gohl, D. M., Thiede, J. M., Chacon, J. M., Harcombe, W. R., Maruyama, F., *et al.* (2019) Genomewide assessment of Mycobacterium tuberculosis conditionally essential metabolic pathways. *mSystems* **4**, e00070-19
100. Gupta, M., Sajid, A., Arora, G., Tandon, V., and Singh, Y. (2009) Forkhead-associated domain-containing protein Rv0019c and polyketide-associated protein PapA5, from substrates of serine/threonine protein kinase PknB to interacting proteins of Mycobacterium tuberculosis. *J. Biol. Chem.* **284**, 34723–34734
101. Grasser, K. D., Grimm, R., and Ritt, C. (1996) Maize chromosomal HMGc. Two closely related structure-specific DNA-binding proteins specify a second type of plant high mobility group box protein. *J. Biol. Chem.* **271**, 32900–32906
102. Singha, B., Behera, D., Khan, M. Z., Singh, N. K., Sowpati, D. T., Gopal, B., *et al.* (2023) The unique N-terminal region of Mycobacterium tuberculosis sigma factor A plays a dominant role in the essential function of this protein. *J. Biol. Chem.* **299**, 102933